



## Thermodynamic analysis of an absorption-assisted multi-effect thermal desalination system with an extended operating temperature range

Yongqing Wang<sup>a,b,c,\*</sup>, Shaohui Yang<sup>a,b,c</sup>

<sup>a</sup>College of Mechanical and Energy Engineering, Jimei University, Xiamen, 361021, China, Tel. +86 592 6180597; Fax: +86 592 6183523; emails: yongqing@jmu.edu.cn (Y. Wang), yangshaohui1979@163.com (S. Yang)

<sup>b</sup>Key Laboratory of Energy Cleaning Utilization and Development of Fujian Province, Xiamen, 361021, China

<sup>c</sup>Key Laboratory of Ocean Renewable Energy Equipment, Fujian Province University, Xiamen, 361021, China

Received 3 September 2018; Accepted 27 January 2019

### ABSTRACT

This study presents a thermodynamic analysis of an absorption-assisted multi-effect evaporation (MEE) water desalination system, ABMEE. Compared with the conventional MEE systems operating within 40°C~70°C, the MEE subsystem in ABMEE has a greatly extended operation temperature range of 10°C~70°C, thus being able to accommodate up to nine more effects. Since the temperatures of the discharged brine and the distillate from the last effect of MEE are lower than the ambient temperature, the system produces refrigeration as by-product. Owing to the coupling with the absorption unit, a water production gain up to 36% can be obtained compared with a baseline 9-effect MEE system, and an energy saving rate up to 53% can be obtained when the produced refrigeration is also considered. A detailed parametric sensitivity analysis is performed by analyzing the influence of the main factors on the water production, refrigeration production and energy saving benefit of ABMEE. The upper and lower limits of the motive steam saturation temperature, within which the ABMEE system can operate, are illustrated for different conditions. In the situations where the produced refrigeration is not needed, it can be used to enhance the water production of ABMEE by using it to cool the feed seawater of the added effects of MEE, and a 5.1%~8.1% water production gain can be obtained.

*Keywords:* Multi-effect evaporation water desalination; Absorption refrigeration; Thermodynamic performance; Extended temperature range

### 1. Introduction

Industrial desalination of seawater and brackish water has become an important way of mitigating water shortages in many arid areas in the world. It is reported that the global cumulative online capacity of desalination plants had reached 88.6 million m<sup>3</sup>/d by June 2016 [1]. Reverse osmosis (RO), multi-stage flash (MSF) and low-temperature multi-effect evaporation (LT-MEE) are three most commonly used desalination processes, among which the former one is mechanically driven and the latter two are thermally driven. RO has been increasing its market share in recent years because it is basically more energy-efficient, more compact,

and more flexible in operation and design than thermal desalination [2,3]. Thermal desalination becomes more attractive in the areas where the feedwater has high salinity and/or poor quality, because it produces fresh water through evaporation and condensation processes and is therefore much less sensitive to the salinity and quality of feedwater than RO. Another distinct advantage of thermal desalination is that it mainly consumes low-grade heat, thus suitable to be combined with power generation or other thermal processes to improve the total energy efficiency.

LT-MEE with a top brine temperature (TBT) lower than 70°C has attracted attention during the past two decades, mainly because of its lower scaling and corrosion rates,

\* Corresponding author.

lower capital cost, longer operation life and less pumping power consumption [4] compared with MSF. In a LT-MEE system, the vapor formed in one effect is used as the driving heat source of the next effect, so increasing the number of effects can lead to significantly improved performance of water production. For example, in a case study in [5], increasing the number of effects from 5 to 8 increased the performance ratio PR (defined as the mass ratio of the produced water and the motive steam) from 4.1 to 6.1, increased by 49%. However, limited by the allowable TBT (which is determined by controllable scaling and fouling) and the final condensing temperature (which is determined by the ambient conditions), the operating temperature range of the effects in LT-MEE is usually within 40°C–70°C, limiting the increase of the number of effects. For example, setting the inter-effect temperature difference at a typical value of 3.5°C, the maximum number of effects that can be obtained is 9.

In order to raise the number of effects of LT-MEE, Aly [6] creatively proposed using an absorption cooling machine to establish a low-temperature environment for LT-MEE, thus lowering the operating temperature of the last effect from around 40°C to 6°C. With a TBT of 63°C and an inter-effect temperature difference of 3°C, a 20-effect LT-MEE was configured. The proposed system was predicted to have a PR of 14.2 for water production, plus a by-product of cooling capacity derived from the last-effect blowdown with a temperature of 6.5°C. Thu et al. [7] proposed a system composed of an adsorption cycle and a LT-MEE desalination unit, where the final condensing temperature dropped to 5°C–10°C and up to four effects were added. The water production rate was more than twice compared with a conventional 8-effect MEE driven by the same hot water at 75°C, and more than 40% of the increase was attributed to the effects operating below the ambient temperature (30°C). Shahzad et al. [8,9] studied a similar system where the operating temperature of the last effect was 3°C, and verified the effectiveness of the system experimentally. It should be noted that in the adsorption based systems, the parameters such as the temperature and the water production rate of each effect of LT-MEE change cyclically because the adsorption and desorption processes occur alternately.

The studies [6–9] conducted so far reveal that, by using absorption or adsorption cycle, the operating temperature range of LT-MEE can be extended significantly and thereby more effects can be accommodated, and the result is significantly improved performance over conventional LT-MEEs. Considering that the absorption technology is much more mature than the adsorption technology, we focus our efforts on an absorption-assisted LT-MEE system, ABMEE, in this paper. Although, the ABMEE system studied is also integrated by a LiBr-H<sub>2</sub>O absorption unit and a MEE unit, this study differs significantly from [6]: first, this study is a detailed thermodynamic analysis other than a conceptual proposal and case study [6], providing details of parametric sensitivity, parameters selection and system performance; second, the situation where the refrigeration produced by ABMEE is not needed anywhere, is considered and the possibility of using the refrigeration to enhance the water production of ABMEE is discussed.

## 2. System configuration

The ABMEE system is composed of two subsystems: a single-effect LiBr-H<sub>2</sub>O absorption unit and a LT-MEE water desalination unit, with the configuration schematically shown in Fig. 1. The two subsystems are interconnected: the steam generated in the generator of the absorption unit enters the first effect of MEE, serving as the driving heat source for desalination, and the LiBr-H<sub>2</sub>O solution in the absorber absorbs the water vapor formed in the last effect of MEE, creating a low-pressure and then low-temperature environment for MEE. The MEE subsystem is divided into two sections: the higher-temperature section (HS) operating within the same temperature range as a conventional LT-MEE, and the lower-temperature section (LS) operating within a lower temperature range than a conventional LT-MEE.

The motive steam (1) heats the LiBr-H<sub>2</sub>O mixture in the generator and boils off part of the water in it. The generated steam (4) is routed into a desuperheater, where its sensible heat, together with part of the sensible heat of the condensate of the motive steam, is used to evaporate the condensate (8) from the flashing box F<sub>1</sub> to produce additional heating steam for MEE. The heating steam (5), whose mass flow rate  $m_5 = m_4 + m_8$ , enters the first evaporator E<sub>1</sub> of MEE, releasing its latent heat for seawater evaporation, and the condensate (6) enters the flashing box F<sub>1</sub> where a small amount of vapor (9) flashes off because of a pressure drop. The vapor (7) evaporated from the seawater in E<sub>1</sub> passes through the preheater H<sub>1</sub> to preheat feed seawater, and then, together with the flashing vapor (9) from F<sub>1</sub>, enters the evaporator E<sub>2</sub>. This process is repeated for all the effects of HS until the last one (the *m*th effect).

Part of the vapor (10) formed in the *m*th effect is routed into the end condenser, and the balance (11) enters the evaporator E<sub>*m+1*</sub>, serving as the heating steam of the LS. The LS doesn't contain seawater preheaters because the temperature of the feed seawater (15) is higher than the operating temperature of most evaporators. The vapor (16) formed in the last effect (the *n*th effect) of LS is absorbed by the LiBr-H<sub>2</sub>O solution in the absorber. The weak solution (17) is preheated in the solution heat exchanger and then heated in the generator to generate steam (4). Because the temperatures of the concentrated brine (14) and the distillate (13) from the *n*th effect are lower than the ambient temperature, the system produces refrigeration as by-product.

## 3. Calculation conditions and performance criteria

### 3.1 Calculation conditions

The main calculation conditions and assumptions are summarized in Table 1. Following the mass and energy conservation principles, we built the governing equations of mass balance, involving the mass balance of each species of the solutions, and energy balance for each component and the entire system. The simulation was carried out using the Engineering Equation Solver (EES) software [10]. The properties of LiBr-H<sub>2</sub>O solution and steam/water were taken from the correlations provided by EES. The enthalpy of seawater/brine was taken from [11], and the boiling point elevation from [12]. In accordance with industrial practice [13], the

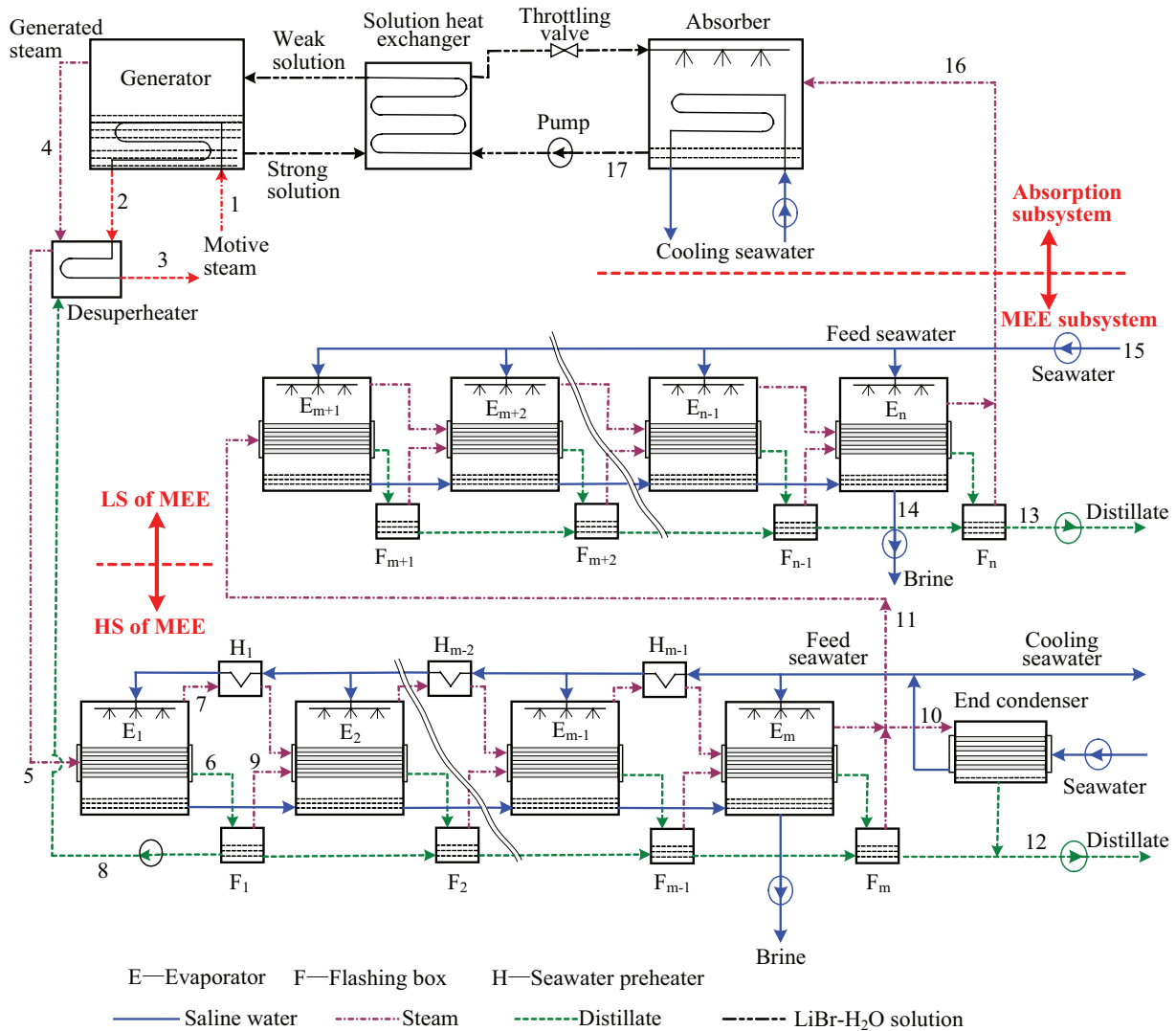


Fig. 1. Schematic diagram of the ABMEE system considered in this study.

evaporators in the HS and those in the LS were considered having the same heat transfer areas, respectively.

The computerized model was first validated by checking the relative errors of mass and energy balance of each component and the whole system, where they were found to be less than  $10^{-6}$ . Because the absorption subsystem and the MEE subsystem are relatively independent, the model of ABMEE was then validated by comparing the simulation results of the two subsystems separately with those in literature [14–16] under the same calculation conditions. The results show that the model predictions compared well with the published data. For example, the relative differences of the coefficient of performance (COP) of the absorption unit and the PR of the MEE unit are both within 3%.

### 3.2. Performance of the baseline MEE system

For the sake of comparison, the conventional 9-effect LT-MEE system is taken as the baseline system, whose configuration is the same as the HS shown in Fig. 1. The calculation conditions for the MEE subsystem (Table 1)

are also used in the modelling of the baseline system. The motive steam is assumed to be saturated, and Fig. 2 shows the influence of its temperature  $T_{ms}$  on the performance ratio of the baseline system,  $PR_0$ .

It is revealed that the baseline MEE has a  $PR_0$  of 8.1~8.4 when  $T_{ms} = 90^{\circ}\text{C} \sim 150^{\circ}\text{C}$ . Despite the fact that the latent heat of condensation of the motive steam decreases with the increase of  $T_{ms}$ , the  $PR_0$  increases with  $T_{ms}$  slightly. The main reason is that not only the latent heat, but also part of the sensible heat of the motive steam is utilized in the desalination process (the saturated motive steam becomes subcooled water when flowing out of the MEE system). Increasing  $T_{ms}$  leads to increased sensible heat available and then slightly increased thermal energy for desalination, and the result is slightly increased  $PR_0$ .

### 3.3. Performance criteria

Performance ratio PR, the most commonly used criterion for evaluating the performance of thermal desalination systems, is also used for ABMEE:

Table 1  
Main calculation conditions and assumptions for the modeling of ABMEE system

Ambient conditions	
Temperature	30°C
Pressure	101.325 kPa
Salinity of seawater	35,000 ppm
MEE subsystem	
Salinity of discharged brine	70,000 ppm
Salinity of fresh water produced	0 ppm
Operating (boiling) temperature of the last evaporator of HS	≥40°C
Temperature difference at the hot side of end condenser	5°C
Operating (boiling) temperature of the last evaporator of LS	≥6°C
Temperature difference at the cold side of desuperheater	10°C
Temperature rise of feed seawater in preheater	3.4°C
Average inter-effect temperature difference	3.4°C
Absorption subsystem	
Mass flow rate of motive steam	1 kg/s
Generator approach temperature	10°C
Absorber approach temperature	5°C
Temperature difference at the cold side of solution heat exchanger	10°C
Temperature difference between strong solution and crystallization point	≥15°C
Mass concentration of strong LiBr-H <sub>2</sub> O solution	≤65%

$$PR = (m_{12} + m_{13}) / m_1 \quad (1)$$

When the mass flow of the motive steam is taken as 1 kg/s (Table 1), the water production rate  $m_w$  equals to the PR numerically. For HS and LS,

$$PR_{HS} = m_{12} / m_5 \quad (2)$$

$$PR_{LS} = m_{13} / m_{11} \quad (3)$$

Although ABMEE is a water and refrigeration cogeneration system, priority should be given to water production when analyzing and designing it, because water production is the main purpose of it. However, as a useful output, the production of refrigeration (denoted by  $q_R$  when 1 kg/s motive steam is consumed) can help achieve better energy utilization. The energy saving rate  $\xi$  is used to evaluate the energy benefit of cogeneration:

$$\xi = m_{LT-MEE} + m_{AR} - 1 \quad (4)$$

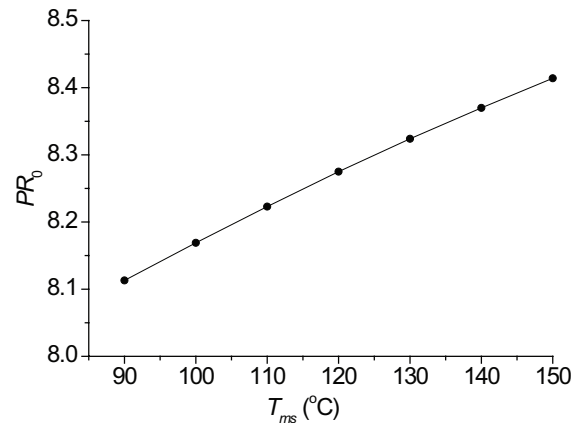


Fig. 2.  $PR_0$  of the baseline 9-effect MEE system.

where  $m_{LT-MEE}$  and  $m_{AR}$  are the mass of the motive steam needed in the water-only baseline LT-MEE system and the conventional refrigeration-only single-effect LiBr-H<sub>2</sub>O absorption refrigerator (AR), respectively, for producing the same amount of fresh water  $m_w$  and refrigeration  $q_R$  as the ABMEE system at the same motive steam conditions.  $\xi$  can also be written as

$$\xi = \xi_1 + \xi_2 = \left( \frac{PR}{PR_0} - 1 \right) + \frac{q_R}{COP \cdot r_m} \quad (5)$$

where  $\xi_1$  is the energy saving rate caused by the improvement in the PR of ABMEE over the baseline MEE, and  $\xi_2$  is that caused by the production of refrigeration; COP is the coefficient of performance of the refrigeration-only AR, and  $r_m$  is the latent heat of condensation of the motive steam.

It should be noted that, unlike the conventional AR where the refrigerant absorbs heat under a nearly constant temperature—the evaporation temperature, the two cold fluids (streams 13 and 14 in Fig.1) from the ABMEE absorb heat by increasing their temperatures. Theoretically, the produced refrigeration corresponding to 1 kg/s motive steam can be calculated by

$$q_{Rth} = [m_{14}(h_{b0} - h_{14}) + m_{13}(h_{w0} - h_{13})] / m_1 \quad (6)$$

where  $h_{b0}$  and  $h_{w0}$  are the specific enthalpy of concentrated brine and fresh water at ambient conditions, respectively. It is impossible to utilize  $q_{Rth}$  totally because temperature differences inevitably exist in the heat-transfer processes between the cold fluids and the medium being cooled. For example, assuming that the cold fluids are used for air conditioning, they would be heated by the room air to a temperature (say 20°C) lower than the room air. So the energy saving rate  $\xi$  is related to what the refrigeration is used for.

In order to illustrate the energy benefit of cogeneration, we assume that the cold fluids absorb heat until their temperatures increase to 20°C, during which the refrigeration output corresponding to 1 kg/s consumed motive steam is

$$q_R = [m_{14}(h_{b,20^\circ C} - h_{14}) + m_{13}(h_{w,20^\circ C} - h_{13})] / m_1 \quad (7)$$

To calculate the  $m_{AR}$  in Eq.(4) and  $\xi_2$  in Eq.(5), we assume that  $q_R$  is produced by a conventional AR with an evaporation temperature of 17°C, with the other calculation conditions the same as those shown in Table 1 for the absorption subsystem. This case study provides a concrete example of the energy saving effect of ABMEE, as illustrated in Section 4.

## 4. Results and discussion

### 4.1. Base-case performance

Table 2 shows the main parameters and thermodynamic performance of the base-case of ABMEE, where the temperature  $T_{ms}$  of the saturated motive steam is taken as 135°C, the number of effects of HS and LS,  $n_{HS}$  and  $n_{LS'}$  are both 9, and the other calculation conditions are taken from Table 1. Compared with the baseline MEE system, the boiling temperature of the last effect of MEE decreases from 41°C to 10.8°C, and the number of effects increases from 9 to 18 owing to the coupling with the absorption unit. Correspondingly, the PR increases from 8.35 to 11.24, increased by 34.6%, and the energy saving rate is 52.9% when the cooling effect is considered.

Although, the HS and the LS both have 9 effects, the LS has a much higher PR than the HS, 10.43 to 8.06 in the base case, for which the main reasons are three: first, in most of the evaporators of LS, the boiling temperature of seawater is lower than the temperature  $t_{15}$  of feed seawater, making it unnecessary to use seawater preheaters, and the result is that more heat is used to evaporate seawater and extra vapor is produced; second, feed seawater flashes in the evaporators operating below  $t_{15'}$  producing more extra vapor; third, the extra vapor produced in one effect serves as a part of the heating steam for the next effect, causing the vapor production to increase at a distinctly increasing rate in the evaporators operating below  $t_{15}$  (Fig. 3), and the result is an obviously increased  $PR_{LS}$ . For example, in the base case ABMEE (Table 2), effects 13–18 of MEE (i.e. effects 4–9 of LS) operate at 28.9°C to 10.8°C, lower than the 30°C of the feed, and the water production rate is 0.43 kg/s in effect 13 and 0.69 kg/s in effect 18, increased by 61%. Different from the LS, the HS operates like a conventional LT-MEE unit, where the heat consumed in the preheaters, and the heat consumed in heating the seawater to its boiling temperature, reduce the heat available for seawater evaporation, and the results is diminished water production in each effect (Fig. 3) and then a much lower  $PR_{HS}$  than  $PR_{LS}$ .

Compared with the baseline MEE which has a  $PR_0$  of 8.35, 9-effect LS with a much higher  $PR_{LS}$  of 10.43 is added to ABMEE, so the PR of ABMEE is expected to be double. However, the calculation results (Table 2) show that it only increases by 34.6%, for which the reason is analyzed below. In the 0.85 kg/s heating steam (stream 5 in Fig. 1) for MEE, 0.72 kg/s (stream 4) is from the generator, which equals to the mass flow of the water vapor (stream 16) produced in the last effect of LS. To ensure this mass balance, only 58% of the water vapor (stream 11) from the last effect of HS is used as the heating steam of LS, and the remainder (stream 10) is routed into the end condenser. The result is that the LS produces much less water than the HS although it has much higher PR; for example, in the base case, the HS is driven by

0.85 kg/s heating steam and produces 6.81 kg/s fresh water, accounting for 60.6% of the total water production, and the LS is driven by 0.42 kg/s heating steam and produces 4.43 kg/s fresh water, accounting for only 39.4% of the total water production. It is thus clear that the requirement of mass balance ( $m_{16} = m_4$ ), and the feature of LS in which the produced vapor increases at an obviously increasing rate in the sequential effects (Fig. 3), make it impossible to fully utilize the advantage of high PR of LS, thus limiting the increase of PR of ABMEE.

The cold fluids (streams 13 and 14) from ABMEE have many possible uses, such as the heat sink of an air conditioning process and the cooling medium of a power plant. However, a typical situation exists where the produced refrigeration is not needed anywhere, for which we propose using the refrigeration to enhance the water production of ABMEE. This sounds strange but works. The most understandable example is using the cold fluids to cool the feed seawater or the heating steam of the  $n$ th effect (the last effect) to reduce the formed vapor  $m_{16'}$  and at the same time, increasing the mass flow  $m_{11}$  of the heating steam for LS to increase the formed vapor  $m_{16}$ ; the result is that, except the  $n$ th effect whose water production  $m_{16}$  remains constant to satisfy the mass balance mentioned above ( $m_{16} = 0.72$  kg/s in the base case), all the other effects in LS get increased water production because of the increased  $m_{11}$ , thus causing increased water production from LS and then higher PR of ABMEE. A number of possible schemes exist because the cold fluids can also be used to cool the feed seawater and/or the heating steam of the other effects of LS. Taking the minimum temperature difference between the cold fluids and the feed seawater or heating steam as 4°C, we calculated the performance of all the possible schemes, and the results show that (1) all the possible schemes, where the refrigeration is consumed by the system itself and only fresh water is produced, have higher PR than the ABMEE outputting both water and refrigeration, and (2) the scheme where the cold fluids are used to cool the feed seawater (stream 15) of LS provides the highest PR—this scheme is referred to as “water-only ABMEE system” below. In the base-case conditions, the water-only ABMEE has a PR of 11.9, which is 6.3% higher than the cogeneration ABMEE. It is thus clear that, in the conditions where the refrigeration is not needed anywhere, it is sensible to use it to enhance the water production of ABMEE by simply adding a heat exchanger between the cold fluids and the feed seawater of LS.

### 4.2. Parametric sensitivity analysis

Under the specified ambient conditions, the main factors influencing the thermal performance of ABMEE are the numbers of effects of HS and LS,  $n_{HS}$  and  $n_{LS'}$  and the temperature of saturated motive steam,  $T_{ms}$ . The influence of the factors is discussed below, with the other conditions kept constant at the base-case values shown in Table 1.

#### 4.2.1. Influence of the numbers of effects $n_{HS}$ and $n_{LS}$

Fig. 4 shows the water production  $m_w$ , the refrigeration production  $q_{Rth}$  and  $q_{Rv}$  and the energy saving rates  $\xi_1$ ,  $\xi_2$  and  $\xi_v$  of the cogeneration ABMEE system for different  $n_{HS}$  and  $n_{LS}$  when  $T_{ms} = 125^\circ\text{C}$ . The PR of ABMEE has the same value

Table 2  
Main parameters and thermodynamic performance of the base-case ABMEE system

Absorption subsystem	$T$ (°C)	$p$ (kPa)	$m$ (kg/s)	$X$ (% LiBr)		
Motive steam	135	312.9	1	0		
Strong solution from generator	125	31.98	4.52	61.8		
Strong solution from heat exchanger	47	–	4.52	61.8		
Weak solution from absorber	37	1.23	5.24	53.3		
Weak solution from heat exchanger	96.9	–	5.24	53.3		
Steam produced in generator	115.4	31.98	0.72	0		
Steam absorbed by absorber	10.1	1.23	0.72	0		
MEE subsystem	$T_{con}$ (°C)	$T_{boil}$ (°C)	$m_{con}$ (kg/s)	$m_{feed}$ (kg/s)	$m_{vap}$ (kg/s)	$Q_{eva}$ (kW)
HS of MEE						
Effect 1	70.6	68.2	0.85	1.65	0.83	1,971
Effect 2	67.2	64.8	0.83	1.62	0.81	1,921
Effect 3	63.8	61.4	0.82	1.58	0.79	1,874
Effect 4	60.4	58.0	0.81	1.54	0.77	1,827
Effect 5	57.0	54.5	0.79	1.51	0.76	1,782
Effect 6	53.6	51.1	0.78	1.48	0.74	1,738
Effect 7	50.2	47.7	0.77	1.45	0.72	1,696
Effect 8	46.8	44.4	0.75	1.41	0.71	1,655
Effect 9	43.5	41.0	0.74	1.38	0.69	1,612
LS of MEE						
Effect 10	40.1	38.0	0.42	0.83	0.41	1,021
Effect 11	37.1	35.0	0.42	0.82	0.41	1,001
Effect 12	34.1	32.0	0.41	0.83	0.41	1,002
Effect 13	31.1	28.9	0.42	0.86	0.43	1,023
Effect 14	28.1	25.7	0.44	0.90	0.45	1,065
Effect 15	24.9	22.4	0.46	0.97	0.49	1,131
Effect 16	21.6	18.9	0.50	1.07	0.53	1,225
Effect 17	18.1	15.0	0.55	1.20	0.60	1,356
Effect 18	14.3	10.8	0.62	1.38	0.69	1,536
System performance						
Produced water of HS			6.81 kg/s			
Produced water of LS			4.43 kg/s			
Produced water of ABMEE, $m_w$			11.24 kg/s			
Produced refrigeration $q_{R0}$			680.8 kW			
Produced refrigeration $q_R$			333.2 kW			
PR of HS, $PR_{HS}$			8.06			
PR of LS, $PR_{LS}$			10.43			
PR of ABMEE			11.24			
PR of baseline 9-effect MEE, $PR_0$			8.35			
Energy saving rate caused by improvement in PR, $\xi_1$			34.6%			
Energy saving rate caused by refrigeration production, $\xi_2$			18.3%			
Energy saving rate of ABMEE, $\xi$			52.9%			

as  $m_w$ . The concentrated brine and the distillate from the last effect of LS have slightly different temperatures, and the average temperature  $T_c$  is used to approximately represent the temperature of the cold fluids, as shown in Fig. 4(b).

Fig. 4(a) reveals that for specified  $T_{ms}$  and  $n_{HS}$ , a higher  $n_{LS}$  doesn't always lead to a higher PR, and an optimum  $n_{LS}$  (denoted by  $n_{LS,opt}$ ) exists which leads to the highest PR. For example,  $n_{LS,opt} = 7$  under  $n_{HS} = 9$ , and  $n_{LS,opt} = 8$  under  $n_{HS} = 6, 7$  and  $8$  when  $T_{ms} = 125^\circ\text{C}$ . Calculations show that

with the increase of  $n_{LS}$ ,  $PR_{LS}$  increases significantly (for example, increasing  $n_{LS}$  from 6 to 9 increases the  $PR_{LS}$  from 6.2 to 10.4, increased by 68%), but it seems that the significant increase of  $PR_{LS}$  has an insignificant influence on the PR of ABMEE (Fig. 4(a)), for which the reason is analyzed below. Under specified  $T_{ms}$  and  $n_{HS}$ , the operation pressure and temperature of the generator remain constant, while those of the absorber decrease with increasing  $n_{LS}$ , and the result is decreased mass flow of absorbed vapor,  $m_{16}$ , with further

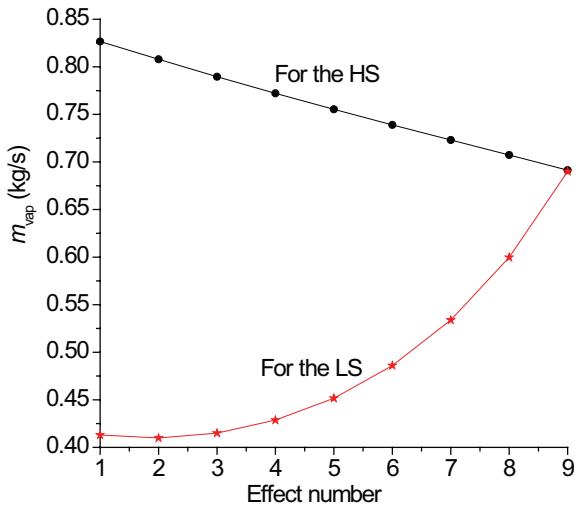


Fig. 3. Water production in each effect in the base-case ABMEE system.

explanation in [17]. The decreased  $m_{16}$  requires a decreased  $m_{11}$ , causing the water production of all the effects of LS, except the new effect(s) added, to decrease. So, although adding a new effect to the LS causes a distinct increase in  $PR_{LS}$ , the water production of LS,  $m_{wLS}$  increases at a much lower rate. For instance, increasing  $n_{LS}$  from 6 to 7 increases the  $PR_{LS}$  by 20.5%, while only increases the  $m_{wLS}$  by 6.7% under  $T_{ms} = 125^\circ\text{C}$  and  $n_{HS} = 8$ . On the other hand, a lowered  $m_{16}$  means a lowered  $m_4$  from the generator and then a lowered  $m_5$  for the HS, resulting in lowered water production of HS,  $m_{wHS}$ . For instance, increasing  $n_{LS}$  from 6 to 7 lowers the  $m_{wHS}$  by 1.7% under  $T_{ms} = 125^\circ\text{C}$  and  $n_{HS} = 8$ . Clearly, the existence of  $n_{LS,opt}$  results from the greatly different influence of  $n_{LS}$  on the performance of HS and LS.

It is also revealed in Fig. 4(a) that for specified  $T_{ms}$  and  $n_{LS}$ , a higher  $n_{HS}$  always leads to a higher PR of ABMEE. Calculations show that adding each effect to the HS causes the PR of ABMEE to increase by 4.2%~8.5% when  $n_{HS} = 6\text{--}9$  and  $n_{LS} = 6\text{--}9$ . Increasing  $n_{HS}$  has only a marginal influence on the performance of LS, so the increase of PR comes from the

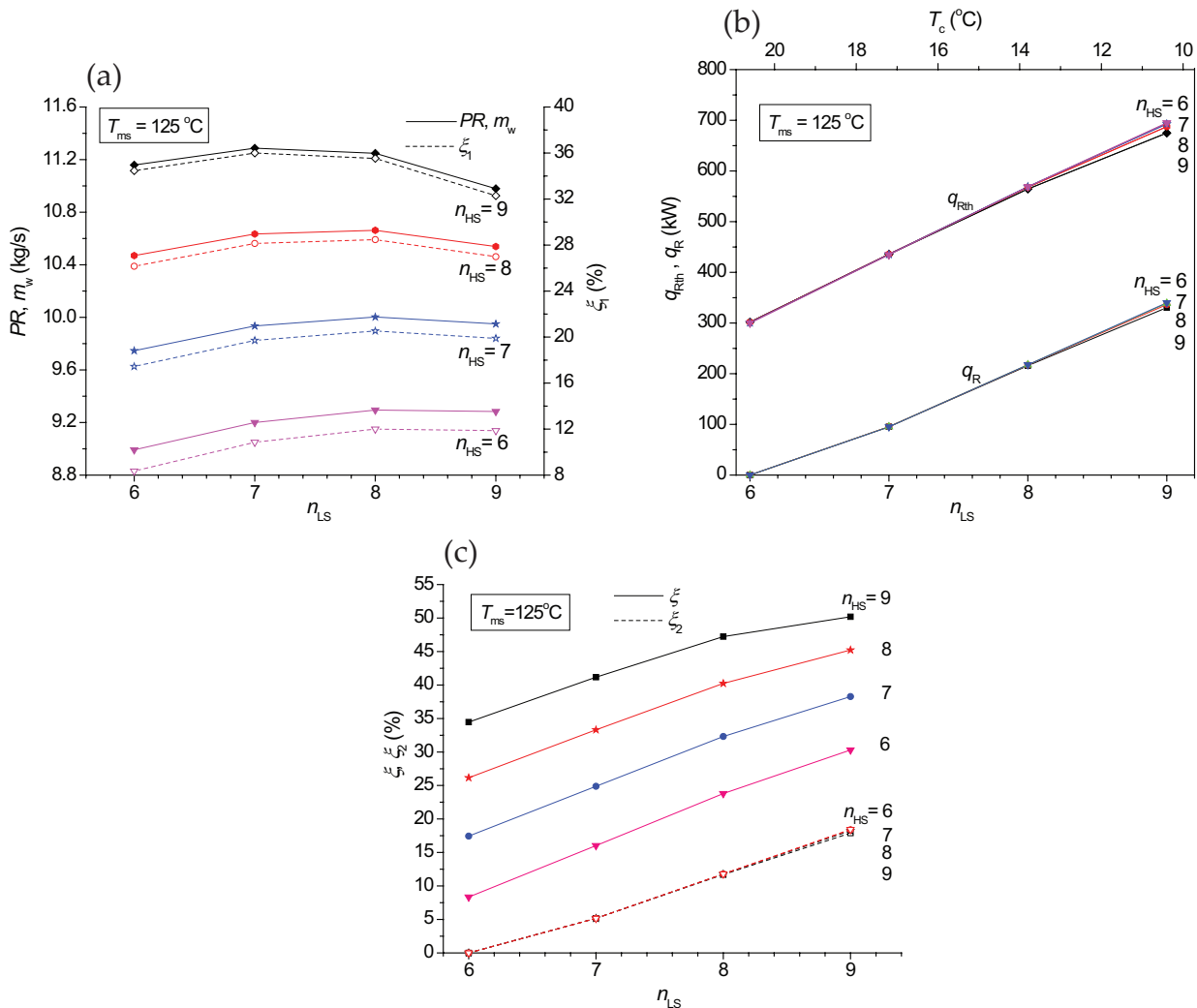


Fig. 4. Influence of the numbers of effects  $n_{HS}$  and  $n_{LS}$  (a) Water production and energy saving rate  $\xi_1$ , (b) Refrigeration production and (c) Energy saving rates  $\xi_2$  and  $\xi$ .

increase of  $m_{wHS}$ . Because of the monotonic influence of  $n_{HS}$  on the PR of ABMEE, the maximum  $n_{HS}$  that can be obtained is also the optimum  $n_{HS}$  corresponding to the highest PR. Under the typical calculation conditions shown in Table 1, the maximum  $n_{HS}$  is 9 (referring to the parameters of HS in the base-case calculation shown in Table 2), and so is the optimum  $n_{HS}$ .

Because  $n_{HS}$  has only a marginal influence on the performance of LS, the produced refrigeration  $q_R$  (or  $q_{Rth}$ ) has only a marginal variation with the increase of  $n_{HS}$  as shown in Fig. 4(c). Contrarily,  $n_{LS}$  has a strong influence on  $q_R$ . When  $T_{ms}$  and  $n_{HS}$  are specified, increasing  $n_{LS}$  leads to a distinct increase in  $q_R$  for two reasons: first, adding each effect to the LS causes the temperatures of the cold fluids to decrease by 3.4°C which is the inter-effect temperature difference used in our calculation (Table 1), and second, increasing  $n_{LS}$  increases  $m_{wLS}$  as mentioned above, and proportionally increase the mass flows of the two cold fluids. So, as illustrated in Fig. 4(c), a higher  $n_{LS}$  leads to not only more  $q_R$  but also lower temperature of  $q_R$ .

It should be noted that the requirements of the maximum PR and the maximum  $q_R$  (or  $q_{Rth}$ ) on the system parameters are different. For example, the maximum PR requires  $n_{HS} = 9$  and  $n_{LS} = 7$ , while the maximum  $q_R$  requires  $n_{HS} = n_{LS} = 9$ , when  $T_{ms} = 125^\circ\text{C}$ . Although, the produced refrigeration is only a by-product of water production, it is beneficial for improving the energetic and economic performance of the whole ABMEE system, because its amount is large. For example, driven by 1 kg/s saturated steam at  $135^\circ\text{C}$ , an ABMEE system with  $n_{HS} = n_{LS} = 9$  can produce 11.24 kg/s of water, and simultaneously 680.8 kW ( $q_{Rth}$ ) or 333.2 kW ( $q_R$ ) of refrigeration. When  $n_{LS}$  is 6, 7, 8 and 9, the temperatures of the cold fluids are around  $20.6^\circ\text{C}$ ,  $17.2^\circ\text{C}$ ,  $13.8^\circ\text{C}$  and  $10.4^\circ\text{C}$ , respectively. It is thus clear that, taking  $n_{HS} = 9$  is always beneficial because it can help obtain the highest water production, while the choice of  $n_{LS}$  depends partially on the water capacity needed and partially on the temperature and the amount of refrigeration needed.

The energy saving rate  $\xi_1$  caused by the improvement of PR certainly has the same trend as PR (Fig. 4(a)), and the energy saving rate  $\xi_2$  caused by the refrigeration production has the same trend as  $q_R$  (Figs. 4(b) and 4(c)). As a result, the energy saving rate  $\xi$  of ABMEE increases with the increase of  $n_{HS}$  and  $n_{LS}$  (Fig. 4(c)).

The  $n_{HS}$  and  $n_{LS}$  have also influence on the range of  $T_{ms}$  within which the ABMEE system can operate. Fig. 5 illustrates the upper and lower limits of  $T_{ms}$  (denoted by  $T_{ms,max}$  and  $T_{ms,min}$  respectively), for different  $n_{HS}$  and  $n_{LS}$ . For instance, the range of  $T_{ms}$  is  $120^\circ\text{C}\sim 143^\circ\text{C}$  when  $n_{HS} = n_{LS} = 9$ , and  $103^\circ\text{C}\sim 135^\circ\text{C}$  when  $n_{HS} = n_{LS} = 7$ . For a specified  $n_{HS}$  which determines the saturation temperature/pressure of the heating steam (stream 5) of HS and then the operating pressure of the generator, a higher  $T_{ms}$  raises the temperature and then the concentration of the strong LiBr-H<sub>2</sub>O solution, making the solution more prone to crystallize and thus restricting the increase of  $T_{ms}$ . Considering the sharp rise of the crystallization temperature of the solution at concentrations higher than 65%, the maximum concentration allowed is usually taken as 65% as done in this study (Table 1), thus determining the upper limit of  $T_{ms}$ . When  $T_{ms}$  decreases, the concentration of the strong solution decreases as well, reducing the concentration difference

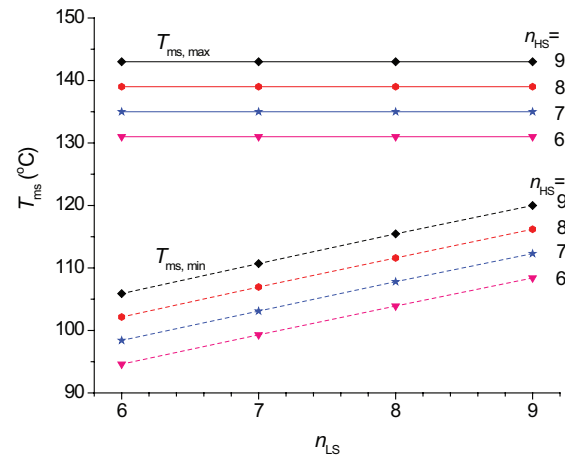


Fig. 5. Upper and lower limits of  $T_{ms}$  for different  $n_{HS}$  and  $n_{LS}$ .

between the strong and weak solutions,  $\Delta X$ . Calculations show that when  $\Delta X < 2\%$ , the PR of ABMEE decreases very sharply with the decrease of  $\Delta X$ , so the minimum  $\Delta X$  allowed is taken as 2% in this paper, which determines the lower limit of  $T_{ms}$ . It is also revealed in Fig. 5 that a lower  $n_{LS}$  leads to a lower  $T_{ms,min}$  and then a wider range of  $T_{ms}$  for which the reason is that a lower  $n_{LS}$  causes a higher absorption pressure  $p_{16}$  and then a lower concentration of weak solution, thus resulting in a lower  $T_{ms,min}$ .

#### 4.2.2. Influence of the motive steam saturation temperature $T_{ms}$

The motive steam is assumed to be saturated, and Fig. 6 shows the influence of its temperature  $T_{ms}$ . Only the system performance under  $n_{HS} = 9$  is illustrated because it can help get the best performance of water production, as discussed in Section 4.2.1. With the increase of  $T_{ms}$ , the PR and  $\xi_1$  of ABMEE (Figs. 6(a) and (b)) first increase at a distinctly diminishing rate and then decrease slowly until the upper limit of  $T_{ms}$  is reached; an optimum  $T_{ms}$  exists which leads to the highest PR and  $\xi_1$ . For instance, for the ABMEE system with  $n_{HS} = n_{LS} = 9$ ,  $T_{ms,opt} = 135^\circ\text{C}$  and the corresponding  $PR_{opt} = 11.2$  and  $\xi_{1,max} = 34.6\%$ .  $T_{ms}$  has an insignificant influence on  $q_R$  and  $\xi_2$  (Figs. 6(c) and (d)), so  $\xi$  (Fig. 6(d)) has a similar trend to PR and  $\xi_1$ . The optimum performance of water production,  $PR_{opt} = 11.3$  and  $\xi_{1,max} = 36.0\%$ , appears when  $T_{ms} = 125^\circ\text{C}$ ,  $n_{HS} = 9$  and  $n_{LS} = 7$ , and the optimum performance of cogeneration,  $\xi_{opt} = 52.9\%$ , appears when  $T_{ms} = 135^\circ\text{C}$  and  $n_{HS} = n_{LS} = 9$ .

The ABMEE system has a good adaptability to varying motive heat source, as reflected in Fig. 6(a), where the PR has only a small variation with  $T_{ms}$  when  $T_{ms}$  varies in a certain range around  $T_{ms,opt}$ . For example, when  $T_{ms} = 125^\circ\text{C}\sim 143^\circ\text{C}$ , PR ranges from 11.24 to 11.3 for the system with  $n_{HS} = 9$  and  $n_{LS} = 8$ , showing a difference less than 0.6%. It is also revealed that the influence of  $n_{LS}$  on the water production of ABMEE becomes insignificant in a certain range of  $T_{ms}$  (Fig. 6(a)). For instance, when  $T_{ms} = 130^\circ\text{C}\sim 143^\circ\text{C}$ , the PR is 11.2~11.3 for  $n_{LS} = 7\sim 9$ , showing a difference less than 1.5%, and when  $T_{ms} = 125^\circ\text{C}\sim 143^\circ\text{C}$ , the PR is 10.98~11.3 for  $n_{LS} = 6\sim 9$ , showing a difference less than 3%. This feature of ABMEE offers certain flexibility for system design.

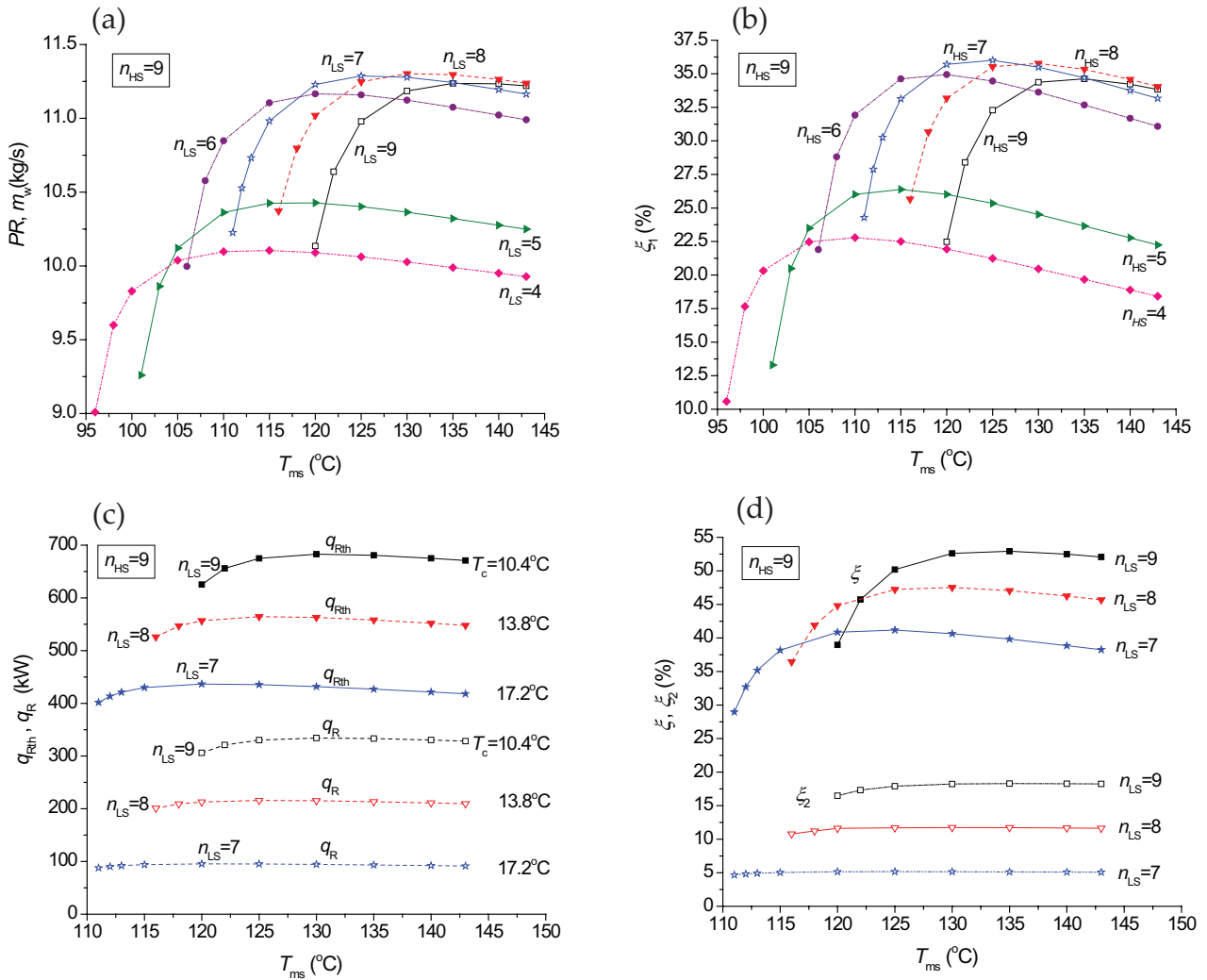


Fig. 6. Influence of the motive steam saturation temperature  $T_{ms}$  (a) Water production (b) Energy saving rate  $\xi_1$  (c) Refrigeration output and (d) Energy saving rates  $\xi_2$  and  $\xi_1$ .

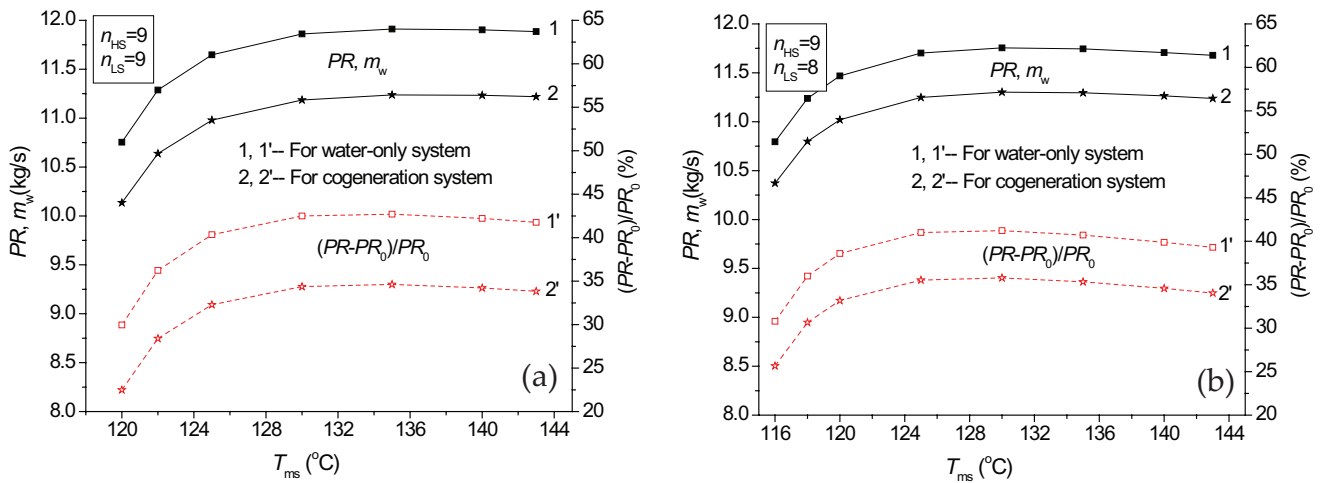


Fig. 7. Improvement of PR of water-only system over cogeneration system (a) Improvement of PR when  $n_{LS}=9$  and (b) Improvement of PR when  $n_{LS}=8$ .

#### 4.2.3. Performance of the water-only ABMEE system

As discussed in Section 4.1, when the produced refrigeration is not needed anywhere, it can be used to enhance the water production of ABMEE by using it to cool the feed seawater of LS. Calculations show that an obvious water production gain, 7.5%–8.1% when  $n_{HS} = 9$  and 5.1%–5.5% when  $n_{LS} = 8$ , can be obtained (Fig. 7). This method is effective only when  $n_{LS}$  is higher, say 8 or 9, because the lower-temperature fluids under higher  $n_{LS}$ , 10.4°C for  $n_{LS} = 9$  and 13.8°C for  $n_{LS} = 8$ , can produce better cooling effect on the feed seawater of LS.

### 5. Conclusions

This study presents a thermodynamic analysis of an absorption-assisted multi-effect evaporation (ABMEE) water desalination system. Owing to the coupling with the absorption unit, the MEE unit operates within a greatly extended temperature range and accommodates much more stages than a conventional MEE. Besides water production, the cold fluids from the last effect of MEE provide refrigeration as by-product. Driven by 105°C–143°C of saturated steam, a water production gain up to 36% can be obtained compared with the baseline 9-effect MEE system, and an energy saving rate up to 53% can be obtained when the produced refrigeration is also considered.

The motive steam saturation temperature  $T_{ms}$  and the numbers of effects,  $n_{HS}$  and  $n_{LS}$ , of the two sections of the MEE subsystem are the main factors influencing the performance of ABMEE. The parametric analysis shows that: adding each effect to the HS causes the PR of ABMEE to increase by 4.2%–8.5%; the maximum  $n_{HS}$  that can be obtained is 9, which is also the optimum  $n_{HS}$  corresponding to the highest PR; for specified  $T_{ms}$  and  $n_{HS}$ , an optimum  $n_{LS}$  (which is not the maximum  $n_{LS}$ ) exists which leads to the highest PR;  $n_{HS}$  has a marginal influence on the cooling capacity; a higher  $n_{LS}$  leads to not only higher cooling capacity but also lower temperature of it; in a certain range of  $T_{ms}$ , the PR of ABMEE only varies slightly with  $T_{ms}$ , indicating a good adaptability of the system to varying motive heat source. The  $n_{HS}$  and  $n_{LS}$  have also influence on the range of  $T_{ms}$  within which the ABMEE system can operate, and the upper and lower limits of  $T_{ms}$  are illustrated in the paper. When the produced refrigeration is not needed anywhere, it can be used to enhance the water production of ABMEE by using it to cool the feed seawater of LS, and calculations show that an obvious water production gain, 7.5%–8.1% when  $n_{HS} = 9$  and 5.1%–5.5% when  $n_{LS} = 8$ , can be obtained.

The lower-temperature section added to the MEE subsystem of ABMEE has much higher PR than the conventional MEEs, but the advantage is not fully utilized in the present layout. Further study is necessary to find more favorable layouts.

### Acknowledgements

The authors gratefully acknowledge the support of the Natural Science Foundation of Fujian Province, China (Project No. 2016J01245).

### Symbols

COP	— Coefficient of performance
$h$	— Specific enthalpy, kJ/kg
$m$	— Mass flow rate, kg/s
$m_w$	— Water production rate corresponding to 1 kg/s motive steam, kg/s
$n$	— Number of effects
$p$	— Pressure, kPa
PR	— Performance ratio
$Q$	— Heat load, kW
$q_R$	— Produced refrigeration corresponding to 1 kg/s motive steam, kW
$q_{Rth}$	— Maximum refrigeration corresponding to 1 kg/s motive steam, kW
$r_m$	— Latent heat of condensation of motive steam [kJ/kg]
$T$	— Temperature, °C
$T_c$	— Average temperature of cold fluids, °C
$T_{ms}$	— Saturation temperature of motive steam, °C
TBT	— Top brine temperature, °C
$X$	— Mass concentration of LiBr-H <sub>2</sub> O solution, %
$\xi$	— Energy saving rate of ABMEE, %
$\xi_1$	— Energy saving rate caused by PR improvement of ABMEE, %
$\xi_2$	— Energy saving rate caused by refrigeration production of ABMEE, %

### Abbreviations and subscripts

ABMEE	— Absorption assisted LT-MEE system
AR	— Absorption refrigerator
$b$	— Concentrated brine
boi	— Boiling
con	— Condensate formed inside the tubes of evaporator
$E$	— Evaporator
eva	— Evaporator
$F$	— Flashing box
feed	— Feed seawater
$H$	— Seawater preheater
LT-MEE	— Low temperature multi-effect evaporation
max	— Maximum
MSF	— Multi-stage flash
opt	— Optimum
RO	— Reverse osmosis
HS	— Higher-temperature section of MEE subsystem
LS	— Lower-temperature section of MEE subsystem
vap	— Vapor formed in evaporator
$w$	— Fresh water
0	— Ambient; baseline MEE
1, 2, ...	— States on the system flow sheet

### References

- [1] IDA Desalination Yearbook (2016–2017), <http://www.desalyearbook.com/>.
- [2] A.M. Helal, A.M. El-Nasher, E.B. Al-Katheeri, S. Al-Malek, Optimal design of hybrid RO/MSF desalination plants: part 1 — Modeling and algorithms, *Desalination*, 154 (2003) 43–66.
- [3] C. Gao, G. Chen, *Handbook of Seawater Desalination Technology and Engineering*, Chemical Industry Press, Beijing, 2004 (in Chinese).
- [4] G. Kronenberg, F. Lokiec, Low-temperature distillation processes in single- and dual-purpose plants, *Desalination*, 136 (2001) 189–197.

- [5] Y. Wang, N. Lior, Performance analysis of combined humidified gas turbine power generation and multi-effect thermal vapor compression desalination systems — Part 1: the desalination unit and its combination with a steam-injected gas turbine power system, *Desalination*, 196 (2006) 84–104.
- [6] S.E. Aly, A study of a new vapor compression/multi-effect stack (TVC/MES) low temperature distillation system, *Desalination*, 103 (1995) 257–263.
- [7] K. Thu, Y. Kim, G. Amy, W.G. Chun, K.C. Ng, A synergetic hybridization of adsorption cycle with the multi-effect distillation (MED), *Appl. Therm. Eng.*, 62 (2014) 245–255.
- [8] M.W. Shahzad, K.C. Ng, K. Thu, B.B. Saha, W.G. Chun, Multi effect desalination and adsorption desalination (MEDAD): a hybrid desalination method, *Appl. Therm. Eng.*, 72 (2014) 289–297.
- [9] M.W. Shahzad, K. Thu, Y. Kim, K.C. Ng, An experimental investigation on MEDAD hybrid desalination cycle, *Appl. Energy*, 148 (2015) 273–281.
- [10] F-chart Software, <http://www.fchart.com/ees/ees.shtml/>.
- [11] Y. Wang, N. Lior, Proposal and analysis of a high-efficiency combined desalination and refrigeration system based on the LiBr-H<sub>2</sub>O absorption cycle — Part 1: system configuration and mathematical model, *Energy. Convers. Manage.*, 52 (2011) 220–227.
- [12] M.H. Sharqawy, J.H. Lienhard V, S.M. Zubair, Thermophysical properties of seawater: a review of existing correlations and data, *Desal. Wat. Treat.*, 16 (2010) 354–380.
- [13] H.T. El-Dessouky, H.M. Ettouney, *Fundamentals of Salt Water Desalination*, Elsevier, Amsterdam, 2002.
- [14] G.A. Florides, S.A. Kalogirou, S.A. Tassou, L.C. Wrobel, Design and construction of a LiBr water absorption machine, *Energy. Convers. Manage.*, 44 (2003) 2483–2508.
- [15] F.N. Alasfour, M.A. Darwish, A.O. Bin Amer, Thermal analysis of ME-TVC+MEE desalination systems, *Desalination*, 174 (2005) 39–61.
- [16] C. Wang, Performance analysis of low-temperature multi-effect evaporation seawater desalination plants, Master's thesis, North China Electric Power University, 2006 (in Chinese).
- [17] Y. Dai, Technology and application of lithium bromide absorption refrigeration, Mechanical Industry Press, Beijing, 2002 (in Chinese).